

JOINT DUAL-DOMAIN MATRIX FACTORIZATION FOR ECG BIOMETRIC RECOGNITION

Kuikui Wang¹, Gongping Yang^{1,2*}, Yuwen Huang², Lu Yang³, Yilong Yin¹

¹ School of Software, Shandong University, Jinan 250101, China

² School of Computer, Heze University, Heze 274015, China

³ School of Computer Science and Technology, Shandong Jianzhu University, Jinan 250101, China

ABSTRACT

Electrocardiogram (ECG) biometrics has aroused extensive attention in the research field of biometric recognition. However, most existing methods either only consider a single domain (time domain or frequency domain) to extract features or extract multi-features while ignoring the specific properties of each domain. In this paper, we propose a novel ECG biometrics framework termed Joint Dual-domain Matrix Factorization (JDMF). JDMF learns latent spaces for each domain by exploring the cross-correlations between them and preserving domain-specific properties. To endow the latent spaces with more powerful representation capabilities, JDMF further makes full use of the supervised information and could automatically learn the weights of domains. The experimental results on two widely-used datasets indicate that the proposed framework can outperform state-of-the-arts.

Index Terms— ECG, Biometric Recognition, Dual Domain, Matrix Factorization

1. INTRODUCTION

ECG signals consist of a complex frequency and time structure [1] and many previous research works investigate the possibility of processing ECG signals in the time domain and frequency domain. Some existing methods use wavelet features in frequency domain [2, 3, 4]. Some pioneer works [5, 6, 7] extract features based on fiducial points in the time domain, such as distances between fiducial points, amplitudes, angles, areas, slopes, QRS complex, and so on. Although those time-frequency based methods have presented promising results, they only focus on transforming the ECG into the time-frequency domain while failing to synchronously explore the specific properties in each domain and the correlations between two domains [8, 9, 10, 11]. In this paper, we focus on the ECG biometrics joint dual domains and investigate two valuable problems. The first one is how to separately preserve

the specific properties in the time domain and frequency domain. Although each domain could offer specific features, it is much better to collectively learn domain-specific features and make them compatible with each other by simultaneously modeling. Therefore, the second problem is how to validly construct correlations between the domain-specific representations from dual domains.

To tackle the above two issues, we propose a novel framework for ECG biometric recognition, named Joint Dual-domain Matrix Factorization (JDMF). The flow diagram of the proposed framework is shown in Fig. 1. We firstly learn a latent space for each domain with the purpose to preserve the specific properties in each domain by simultaneously factorizing them. Then, the learned latent representations in each domain are connected by a correlation matrix to retain the shared properties. In particular, we embed the semantic information to guide the representation learning and adaptive weights are learned for each domain.

The main contributions of our paper are summarized as follows: 1) We propose a novel joint dual-domain matrix factorization based framework to effectively learn the latent spaces for ECG signals in the time domain and frequency domain, which can also explore the cross-correlations between them. 2) A weight learning scheme is proposed to automatically generate the weights for domains. The weights in each domain are dynamic and enhance the discriminative capabilities of different domain features. 3) Extensive experiments conducted on benchmark datasets demonstrate that the proposed framework outperforms the state-of-the-art.

2. PROPOSED METHOD

2.1. Model Formulation

Assuming that the training set is formed by n samples, the base features extracted in time domain and frequency domain are represented by $\mathbf{X}_t = [\mathbf{x}_1, \mathbf{x}_2, \dots, \mathbf{x}_n] \in \mathbb{R}^{m_1 \times n}$, and $\mathbf{X}_f = [\mathbf{y}_1, \mathbf{y}_2, \dots, \mathbf{y}_n] \in \mathbb{R}^{m_2 \times n}$, where m_1 and m_2 are the dimensionality of the base feature space in time domain and frequency domain, respectively (the generation of base features are presented in Sec 3.1).

* Corresponding author, gpyang@sdu.edu.cn. This work was supported in part by the NSFC-Xinjiang Joint Fund under Grant U1903127, in part by the Natural Science Foundation of Shandong Province under Grant ZR2020MF052, and in part by the National Natural Science Foundation of China under Grant 62076151.

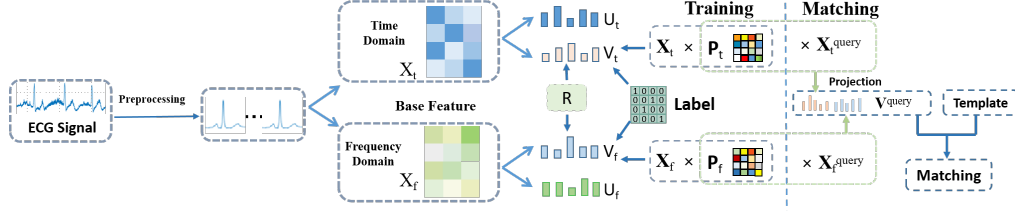


Fig. 1. Flow diagram of proposed framework and matching procedure.

Preserving specific properties. To remove redundant information and distill the most important information of samples from \mathbf{X}_t and \mathbf{X}_f , we could conduct matrix factorization on them respectively:

$$\mathcal{O}_1 = \alpha_t \|\mathbf{X}_t - \mathbf{U}_t \mathbf{V}_t\|_F^2 + \alpha_f \|\mathbf{X}_f - \mathbf{U}_f \mathbf{V}_f\|_F^2, \quad (1)$$

where $\mathbf{U}_t \in \mathbb{R}^{m_1 \times r}$, $\mathbf{U}_f \in \mathbb{R}^{m_2 \times r}$, $\mathbf{V}_t \in \mathbb{R}^{r \times n}$ is the latent representation of samples coming from time domain, $\mathbf{V}_f \in \mathbb{R}^{r \times n}$ denotes the latent features from frequency domain, r is the dimensionality of the latent spaces, and α_t (α_f) is the parameter balancing time domain (frequency domain). With Eq.(1), we can preserve the specific properties of each domain by simultaneously and respectively factorizing them. Although collective matrix factorization could be adopted to make \mathbf{U}_t equal to \mathbf{U}_f , we argue that it is not reasonable to force the time-frequency dual-domain to share the same latent space as the specific properties in each domain may lose.

Constructing correlations. As stated above, we intend to force domain-specific features to be compatible with each other while preserving their distinct properties. Thus, we elaborately build a correlation construction module that connects two latent spaces to retain the shared properties meanwhile preserving specific properties of dual domains:

$$\mathcal{O}_2 = \eta \|\mathbf{V}_t - \mathbf{R} \mathbf{V}_f\|_F^2, \quad (2)$$

where $\mathbf{R} \in \mathbb{R}^{r \times r}$ connects the latent time domain and latent frequency domain, and η is the parameter that controls the contribution of this module. In light of this, the specific representations of time domain and frequency domain are connected by the correlation matrix \mathbf{R} .

Embedding the semantic information. As different individuals have diverse ECG, it is essential to mine effective and unique patterns for individuals and embed them into the latent representations of their samples. To achieve this aim, we try to further embed the semantic information into the learning of latent representations:

$$\mathcal{O}_3 = \theta (Tr(\mathbf{V}_t \mathbf{L}_w \mathbf{V}_t^T) + Tr(\mathbf{V}_f \mathbf{L}_w \mathbf{V}_f^T)), \quad (3)$$

where $\mathbf{L}_w = \mathbf{D} - \mathbf{S}$, $\mathbf{S} = \mathbf{L} \times \mathbf{L}^T$ denotes the pair-wise similarity among all training samples, $\mathbf{L} \in \{0, 1\}^{n \times c}$ is label matrix which reflects that samples belong to which subject, c is the number of subjects, and θ is tradeoff parameter. $\mathbf{L}_{ij} = 1$

if the i -th sample belongs to the j -th subject and 0 otherwise, and \mathbf{D} is a diagonal matrix ($\mathbf{D}(i, i) = \sum_j \mathbf{L}_{i,j}$). With Eq.(3), we can preserve the semantic information and force the latent representations of each subject to be similar.

Projection matrices learning. Finally, we construct projections from base feature spaces to the latent spaces so as to transform the out-of-sample query data into latent spaces:

$$\mathcal{O}_4 = \gamma (\|\mathbf{P}_t \mathbf{X}_t - \mathbf{V}_t\|_F^2 + \|\mathbf{P}_f \mathbf{X}_f - \mathbf{V}_f\|_F^2), \quad (4)$$

where $\mathbf{P}_t \in \mathbb{R}^{r \times m_1}$ and $\mathbf{P}_f \in \mathbb{R}^{r \times m_2}$ are projection matrices, γ is the tradeoff parameter.

Overall Objective Function. By combining Eq.(1), Eq.(2), Eq.(3), and Eq.(4), the overall objective function can be given as follows:

$$\min_{\mathbf{U}_t, \mathbf{U}_f, \mathbf{P}_t, \mathbf{P}_f, \mathbf{V}_t, \mathbf{V}_f, \mathbf{R}} \mathcal{O}_1 + \mathcal{O}_2 + \mathcal{O}_3 + \mathcal{O}_4 + \lambda Re(\mathbf{U}_t, \mathbf{U}_f, \mathbf{P}_t, \mathbf{P}_f, \mathbf{V}_t, \mathbf{V}_f, \mathbf{R}), \quad (5)$$

where $Re(\cdot)$ is regularization term, λ is tradeoff parameter.

2.2. Optimization Algorithm

To solve the optimization problem in Eq.(5), we propose an alternating optimization algorithm with the following steps. By repeating these steps, we can update all variables iteratively until the objective function converges.

Step 1: Update \mathbf{U}_t and \mathbf{U}_f . By fixing other variables, the objective function to learn \mathbf{U}_t and \mathbf{U}_f can be given:

$$\begin{aligned} \min_{\mathbf{U}_t} & \alpha_t \|\mathbf{X}_t - \mathbf{U}_t \mathbf{V}_t\|_F^2 + \lambda \|\mathbf{U}_t\|_F^2, \\ \min_{\mathbf{U}_f} & \alpha_f \|\mathbf{X}_f - \mathbf{U}_f \mathbf{V}_f\|_F^2 + \lambda \|\mathbf{U}_f\|_F^2. \end{aligned} \quad (6)$$

We then set the derivative of Eq.(6) w.r.t. \mathbf{U}_t and \mathbf{U}_f to zero. Then, the solution of \mathbf{U}_t and \mathbf{U}_f can be easily obtained:

$$\begin{aligned} \mathbf{U}_t &= \alpha_t \mathbf{X}_t \mathbf{V}_t^T (\alpha_t \mathbf{V}_t \mathbf{V}_t^T + \lambda \mathbf{I})^{-1}, \\ \mathbf{U}_f &= \alpha_f \mathbf{X}_f \mathbf{V}_f^T (\alpha_f \mathbf{V}_f \mathbf{V}_f^T + \lambda \mathbf{I})^{-1}. \end{aligned} \quad (7)$$

Step 2: Update \mathbf{P}_t and \mathbf{P}_f . Similar with step 1, we set the derivative of \mathbf{P}_t (\mathbf{P}_f) sub-problems w.r.t. \mathbf{P}_t (\mathbf{P}_f) to zero to get the closed-form solutions:

$$\begin{aligned} \mathbf{P}_t &= \alpha_t \gamma \mathbf{V}_t \mathbf{X}_t^T (\alpha_t \gamma \mathbf{X}_t \mathbf{X}_t^T + \lambda \mathbf{I})^{-1}, \\ \mathbf{P}_f &= \alpha_f \gamma \mathbf{V}_f \mathbf{X}_f^T (\alpha_f \gamma \mathbf{X}_f \mathbf{X}_f^T + \lambda \mathbf{I})^{-1}. \end{aligned} \quad (8)$$

Step 3: Update \mathbf{V}_t and \mathbf{V}_f . The objective function to solve \mathbf{V}_t can be rewritten as:

$$\min_{\mathbf{V}_t} \alpha_t (\|\mathbf{X}_t - \mathbf{U}_t \mathbf{V}_t\|_F^2 + \gamma \|\mathbf{P}_t \mathbf{X}_t - \mathbf{V}_t\|_F^2) + \theta \text{Tr}(\mathbf{V}_t \mathbf{L}_w \mathbf{V}_t^\top) + \eta \|\mathbf{V}_t - \mathbf{R} \mathbf{V}_f\|_F^2 + \lambda \text{Re}(\mathbf{V}_t), \quad (9)$$

The closed-form solution can also be obtained by setting the derivative of Eq. (9) w.r.t. \mathbf{V}_t to zero. That is:

$$(2\alpha_t \mathbf{U}_t^\top \mathbf{U}_t + 2(\alpha_t \gamma + \eta + \lambda) \mathbf{I}) \mathbf{V}_t + \theta \mathbf{V}_t (\mathbf{L}_w + \mathbf{L}_w^\top) - (2\alpha_t \mathbf{U}_t^\top \mathbf{X}_t + 2\alpha_t \gamma \mathbf{P}_t \mathbf{X}_t + 2\eta \mathbf{R} \mathbf{V}_f) = 0. \quad (10)$$

Eq.(10) is a typical Sylvester equation and can be efficiently solved by using existing toolbox, *i.e.*, *lyap* function in Matlab. Analogous to \mathbf{V}_t , we can solve \mathbf{V}_f . Due to the page limit, we omit the details.

Step 4: Update \mathbf{R} . Analogous to above steps, by setting the derivative of \mathbf{R} sub-problem, we can get:

$$\mathbf{R} = \eta \mathbf{V}_t \mathbf{V}_f^\top (\eta \mathbf{V}_f \mathbf{V}_f^\top + \lambda \mathbf{I})^{-1}. \quad (11)$$

Step 5: Update α_t and α_f . We denote $\|\mathbf{X}_t - \mathbf{U}_t \mathbf{V}_t\|_F^2 + \gamma \|\mathbf{P}_t \mathbf{X}_t - \mathbf{V}_t\|_F^2$ as g^t for convenience, and $\|\mathbf{X}_f - \mathbf{U}_f \mathbf{V}_f\|_F^2 + \gamma \|\mathbf{P}_f \mathbf{X}_f - \mathbf{V}_f\|_F^2$ is denoted by g^f . The optimal α_t and α_f can be obtained by:

$$\alpha_t = g^t / (g^t + g^f), \quad \alpha_f = g^f / (g^t + g^f). \quad (12)$$

2.3. Matching Process

With the obtained \mathbf{P}_t and \mathbf{P}_f , the learned discriminative representation of ECG template can be generated as $\mathbf{V}_{template} = \begin{bmatrix} \alpha_t \mathbf{P}_t \mathbf{X}_t^{template} \\ \alpha_f \mathbf{P}_f \mathbf{X}_f^{template} \end{bmatrix}$, where $\mathbf{X}_t^{template}$ and $\mathbf{X}_f^{template}$ are ECG templates in time domain and frequency, respectively. The template for each subject is generated by the mean homologous heartbeat in training set. Similarly, the final representations of testing data can be obtained by $\mathbf{V}_{query} = \begin{bmatrix} \alpha_t \mathbf{P}_t \mathbf{X}_t^{query} \\ \alpha_f \mathbf{P}_f \mathbf{X}_f^{query} \end{bmatrix}$. Finally, for each query, we calculate $d_{ij} = \sqrt{(\mathbf{V}_{query}(i) - \mathbf{V}_{template}(j))^2}$, where d_{ij} is the distance between the i -th query sample $\mathbf{V}_{query}(i)$ and the j -th template. If the distance between query i and template j is the smallest, the query sample i is considered to belong to the j -th subject.

3. EXPERIMENTS

3.1. Experimental Setting

Datasets. The PTB [12] includes 549 recordings including 15 simultaneously measured signals: the conventional 12 leads together with the 3 Frank lead ECGs. In this paper, we chose 248 subjects whose range is longer than 100 seconds,

Table 1. Comparisons with base feature.

Domain	Feature	MIT-BIH	PTB
Time	Shape	90.4%	95.4%
Frequency	DCT	89.3%	94.6%
Fusion	Shape+DCT	92.5%	96.9%
JDMF	Shape+DCT	99.29%	98.99%

Table 2. Comparisons with state-of-the-arts on MIT-BIH.

Dataset	Method	Subject Number	Accuracy
MIT-BIH	[16]	30	96.67%
	[17]	10	91.7%
	[18]	47	93.1%
	[19]	47	94.68%
	[20]	47	96.5%
	JDMF	47	99.29%

and every subject utilizes the single lead (I). The MIT-BIH [13, 14] is one of the most used dataset for ECG biometrics and it is obtained from 47 subjects. We applied Pan-Tompkins [15] to detect the R peak, and then ECG signals are isolated into heartbeats, which are centered at the R peaks with a certain number of sampling points from each side of the R peak. For MIT-BIH, one heartbeat is composed of 260 sampling points and there are 460 sampling points for the PTB database.

Evaluation metrics. To evaluate the performance of our method, accuracy is used as the evaluation criterion, which is the percentage of correctly recognized query samples.

Implementation details. In this paper, we extracted base features from time-frequency pairs to serve as the input of our framework. For the feature in the time domain, we used the amplitude of the ECG signal to represent the morphological feature, named Shape. We extracted Discrete Cosine Transform(DCT) as the base feature in the frequency domain. In the proposed method, each sample is represented by a group of two heartbeats and each individual is regarded as one subject. Each subject has nine homologous samples in the training set and another five homologous samples in the testing set. The dimension of latent representation r is set to 90 and 500 on MIT-BIH and PTB, respectively. The balance parameters, γ , θ , η , and λ are selected by a validation procedure in the experiment. Weights α_t and α_f are adaptive and do not need to be manually set. The iterative number of the optimization algorithm is 25. All experiments are conducted on a PC with an Intel i7-4790 3.60 GHz CPU and 16 GB memory.

3.2. Comparisons with Base Feature

To validate the effectiveness of our dual-domain design strategy, we compared our JDMF with the base feature of a single domain. We also provided a baseline called ‘‘Fusion’’ by concatenating features from two domains. The experimental results are summarized in Table 1 and we can observe that:

Table 3. Comparisons with state-of-the-arts on PTB.

Dataset	Method	Subject Number	Accuracy
PTB	[23]	52	100%
	[21]	100	97.1%
	[22]	10	97.5%
	[19]	248	98.19%
	[20]	290	94.9%
	JDMF	248	98.99%

(1) Our JDMF achieves significant improvement compared with base features in a single domain. (2) Our JDMF outperforms the concatenated dual-domain features (“Fusion”). These observations confirm that our proposed dual-domain learning framework is effective and we can conclude that the representation generated by JDMF has better discrimination.

3.3. Comparisons with the State-of-the-arts

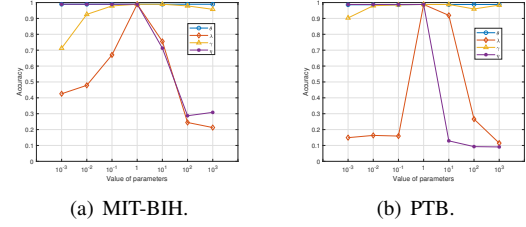
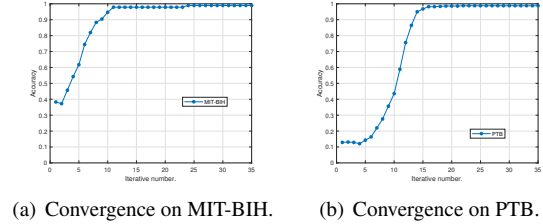
In this section, we made comparisons with existing baselines on two datasets. For MIT-BIH, we compared our method with several state-of-the-art methods, including non-deep approaches [16, 17, 18, 19] and deep learning based method [20]. Experimental results are summarized in Table 2. Based on these results, we have the following observation that the accuracy of our JDMF consistently outperforms the compared baselines in all cases. This is because our method joint time and frequency domains, which is preserving specific properties in each domain, has better representation capability.

For the PTB, the baselines including non-deep methods [21, 22, 19] and deep learning methods [23, 20]. The experimental results are illustrated in Table 3. We can clearly find that our method significantly outperforms most methods. The deep model in [23] obtains a better accuracy. However, its experiments only verified on 52 subjects, and our method has a larger scale of data than it. In addition, the deep method achieves a satisfying performance at the cost of much more training time. To conclude, our method can achieve competitive or even superior performance for ECG biometrics.

3.4. Parameter Sensitivity and Convergence Analysis

In this section, we conducted experiments to analyze the parameter sensitivity. There are several main parameters in our method: (1) α_t and α_f are weights of joint dual-domain matrix factorization; (2) γ controls the projection from base feature to the latent representation; (3) θ controls the terms to embed the semantic information; (4) η controls the correlation between the latent representations to preserve the specific properties; (5) λ is the tradeoff parameter for regularization term. Note that, α_t and α_f are adaptive which means they can be learned without manual interference.

For γ , θ , η , and λ , they vary in the range of [0.001, 1000] and the experimental results are shown in Figure 2. It can be seen that the accuracy is strongly related to the parameters η

**Fig. 2.** Balance parameters γ , θ , η , and λ on two datasets.**Fig. 3.** Convergence on two datasets.

and λ on two datasets. The accuracy maintains satisfactory when η ranges from 0.001 to 1. For the parameter λ , the accuracy achieves best when it is set to 1. It can also be found that JDMF is robust to parameter θ . Besides, our method is robust to γ for a large range. Thus we set γ , θ , η , and λ to 1 in our experiment, respectively. From the above analysis, we can conclude that our proposed framework is easy to tune in practice as only two parameters are sensitive.

We further conducted experiments to validate the convergence of our method. The curves of performance versus iterative number are illustrated in Figure 3. It can be obviously found that, as the iteration number increases, the accuracy monotonically increases and tends to be stable after several iterations. We can observe that the performance achieves the best when the iterative number comes to 25, showing the optimization algorithm could converge quickly.

4. CONCLUSION

In this paper, a joint dual-domain matrix factorization based framework is proposed for ECG biometric recognition. By preserving the specific properties for each domain and constructing cross-correlations between them, the proposed framework could learn discriminative representations. Besides, the latent representations are learned with the guide of labels to embed the semantic information. Furthermore, instead of adopting the fixed weights, the weights in each domain are automatically learned to enhance the flexible capability of the learned latent representations. Extensive experiments on two datasets demonstrate that the proposed framework outperforms the state-of-the-art.

5. REFERENCES

- [1] Yeldos A Altay and Artem S Kremlev, "Comparative analysis of ecg signal processing methods in the time-frequency domain," in *EIconRus*, 2018, pp. 1058–1062.
- [2] M Hejazi, SAR Al-Haddad, YP Singh, SJ Hashim, and AFA Aziz, "ECG biometric authentication based on non-fiducial approach using kernel methods," *Digital Signal Processing*, vol. 52, pp. 72–86, 2016.
- [3] SY Chun, JH Kang, Hanvit Kim, CH Lee, Ian Oakley, and SP Kim, "ECG based user authentication for wearable devices using short time fourier transform," in *TSP*, 2016, pp. 656–659.
- [4] Adrian D. C. Chan, Mohyeldin M. Hamdy, Armin Badre, and Vesal Badee, "Wavelet distance measure for person identification using electrocardiograms," *IEEE Trans. Instrum. Meas.*, vol. 57, no. 2, pp. 248–253, 2008.
- [5] Juan Sebastian Arteaga-Falconi, Hussein Al Osman, and Abdulmotaleb El Saddik, "Ecg authentication for mobile devices," *IEEE Trans. Instrum. Meas.*, vol. 65, no. 3, pp. 591–600, 2015.
- [6] Alex Barros, Denis do Rosário, Paulo Resque, and Eduardo Cerqueira, "Heart of iot: ECG as biometric sign for authentication and identification," in *IWCMC*, 2019, pp. 307–312.
- [7] Anita Pal and Y Narain, "Biometric recognition using area under curve analysis of electrocardiogram," *Int. J. Adv. Comput. Sci. Appl*, vol. 10, no. 1, 2019.
- [8] Rishi Raj Sharma, Mohit Kumar, and Ram Bilas Pachori, "Joint time-frequency domain-based cad disease sensing system using ecg signals," *IEEE Sensors Journal*, vol. 19, no. 10, pp. 3912–3920, 2019.
- [9] Jing Zhang, Jing Tian, Yang Cao, Yuxiang Yang, and Xiaobin Xu, "Deep time-frequency representation and progressive decision fusion for ECG classification," *KBS*, vol. 190, pp. 105402, 2020.
- [10] Grzegorz Kłosowski, Tomasz Rymarczyk, Dariusz Wójcik, Stanisław Skowron, Tomasz Cieplak, and Przemysław Adamkiewicz, "The use of time-frequency moments as inputs of lstm network for ecg signal classification," *Electronics*, vol. 9, no. 9, pp. 1452, 2020.
- [11] Manish Sharma and U. Rajendra Acharya, "A new method to identify coronary artery disease with ECG signals and time-frequency concentrated antisymmetric biorthogonal wavelet filter bank," *PRL*, vol. 125, pp. 235–240, 2019.
- [12] R Bousseljot, D Kreiseler, and A Schnabel, "Nutzung der ekg-signal-datenbank cardiodat der ptb über das internet," *Biomedizinische Technik/Biomedical Engineering*, vol. 40, no. s1, pp. 317–318, 1995.
- [13] G. B. Moody and R. G. Mark, "The impact of the mit-bih arrhythmia database," *IEEE Engineering in Medicine and Biology Magazine*, vol. 20, no. 3, pp. 45–50, 2001.
- [14] AL Goldberger, LA Amaral, L Glass, JM Hausdorff, PC Ivanov, RG Mark, JE Mietus, GB Moody, CK Peng, and HE Stanley, "Physiobank, physiotoolkit, and physionet: components of a new research resource for complex physiologic signals," *Circulation*, vol. 101, no. 23, pp. e215–e220, 2000.
- [15] Jiapu Pan and Willis J Tompkins, "A real-time qrs detection algorithm," *IEEE Trans. Biomed. Eng.*, vol. 32, no. 3, pp. 230–236, 1985.
- [16] M Bassiouni, W Khaleefa, EA El-Dahshan, and ABDEL-BADEEH M Salem, "A machine learning technique for person identification using ecg signals," *Int. J. Appl. Phys.*, vol. 1, pp. 37–41, 2016.
- [17] X Tang and L Shu, "Classification of electrocardiogram signals with rs and quantum neural networks," *International Journal of Multimedia and Ubiquitous Engineering*, vol. 9, no. 2, pp. 363–372, 2014.
- [18] Muhammad Najam Dar, M Usman Akram, Anam Usman, and Shoab A Khan, "Ecg biometric identification for general population using multiresolution analysis of dwt based features," in *InfoSec*, 2015, pp. 5–10.
- [19] Kuikui Wang, Gongping Yang, Yuwen Huang, and Yilong Yin, "Multi-scale differential feature for ECG biometrics with collective matrix factorization," *PR*, vol. 102, pp. 107211, 2020.
- [20] Sara S. Abdeldayem and Thirimachos Bourlai, "A novel approach for ecg-based human identification using spectral correlation and deep learning," *IEEE Trans. Biom. Behav. Identity Sci.*, vol. 2, no. 1, pp. 1–14, 2020.
- [21] Anita Pal and Yogendra Narain Singh, "Ecg biometric recognition," in *ICMC*, 2018, pp. 61–73.
- [22] Joana S Paiva, Duarte Dias, and Joao PS Cunha, "Beatid: Towards a computationally low-cost single heartbeat biometric identity check system based on electrocardiogram wave morphology," *PloS one*, vol. 12, no. 7, pp. e0180942, 2017.
- [23] Ruggero Donida Labati, Enrique Muñoz, Vincenzo Puri, Roberto Sassi, and Fabio Scotti, "Deep-ecg: Convolutional neural networks for ecg biometric recognition," *PRL*, vol. 126, pp. 78–85, 2019.